J. Astrophys. Astr. (2020) 41:11
https://doi.org/10.1007/s12036-020-09630-1

Dust acoustic solitary waves in a five-component cometary plasma with charge variation

A. VARGHESE[1], A. C. SARITHA[1], N. T. WILLINGTON[2], M. MICHAEL[3], S. SEBASTIAN[4], G. SREEKALA[5] and C. VENUGOPAL[1,*]

[1] School of Pure and Applied Physics, Mahatma Gandhi University, Priyadarshini Hills, Kottayam, Kerala 686 560, India.
[2] Department of Physics, C M S College, Kottayam, Kerala 686 001, India.
[3] Department of Physics, Bharata Mata College, Kochi, Kerala 682 021, India.
[4] Department of Physics, S B College, Changanacherry, Kerala 686 101, India.
[5] Department of Physics, S D College, Alappuzha, Kerala 688 003, India.
E-mail: cvgmgphys@yahoo.co.in

MS received 10 November 2019; accepted 20 April 2020

Abstract. We studied dust acoustic solitary waves (DASW) in a five component cometary plasma by deriving the Kadomstev–Petiashvili (KP) equation. The five components consist of two components of electrons described by kappa distributions with different temperatures and spectral indices, a lighter (hydrogen) and a heavier (oxygen) ion component, both ion components are described by Maxwellian distributions. Dust particles, with varying charge, constitute the fifth component. The system supports rarefactive DASWs whose amplitudes are larger when the charges on the dust particles vary. The amplitudes also increase with increasing $z_{d0}n_{d0}$ (product of equilibrium charge number and density of dust) and increasing ion densities. It, however, decreases with increasing spectral indices of the electrons.

Keywords. Charge varying dusty plasma—Lighter and heavier ions—Kappa described electrons—Rarefactive solitary waves.

1. Introduction

A conventional electron–ion plasma is termed a 'dusty plasma' when particles or grains of dust are embedded in it. It has been and continues to be a prominent area of research for the past three decades (Merlino 2014). Research on dust acoustic waves (DAWs) started with its theoretical prediction by Rao *et al*. (1990). The wave was studied using kinetic theory (Rosenberg 1993; Rosenberg 1996; Melandso *et al*. 1993a) and also fluid theory (D' Angelo & Merlino 1996). Experimentally, the very low frequency fluctuations observed from a dusty plasma in a magnetron (Chu *et al*. 1994) was interpreted as DAWs (D'Angelo 1995).

Expansion of the above theoretical studies to dusty plasmas with charge fluctuations was one natural extension (Melandso *et al*, 1993a, b; Varma *et al*. 1993; Jana *et al*. 1993; Bhatt & Pandey 1994); the other was consideration of nonlinear waves. Much progress has been made since the pioneering studies on nonlinear DAWs by Verheest (Verheest 1992) and Rao and Shukla (Rao & Shukla 1994). Extensions, considering various aspects, were very quick: it was found by Mamun and Cairns (1996) that only negative potential structures can exist in a three component plasma of ions, electrons and dust particles. Similarly, the Korteweg–deVries (K–dV) equation was derived to study small, but finite amplitude DAWs in a plasma of a similar composition (Lakshmi *et al.* 1997). Obliquely propagating solitary waves were investigated in a three component dusty plasma by deriving the Zakharov–Kuznetsov equation (Mamun 1998). At about this time, the importance of charge fluctuations on dust particles was realised and the idea was quickly assimilated in a series of studies (Xie *et al*. 1998; Xie

Published online: 23 May 2020

et al. 1999). Nonlinear DAWs were also studied by deriving the modified K–dV (mKdV) equation in a dusty plasma with a trapped ion distribution, two-ion temperature, dust charge fluctuation and dust fluid temperature. Compressive and rarefactive solitary waves and double layers (DL) were also studied (El-Labany *et al*. 2004a).

The first attempt to model a soliton in two dimensions was by Kadomstev and Petiashvili; their effort resulted in the equation now popularly known as the KP equation (Kadomstev & Petviashvili 1970). The KP equation was initially used to study DASW in hot, dusty unmagnetised plasmas (Duan 2002); the equation was extended to the charge varying case also (Duan 2004; El-Labany *et al*. 2004b). These studies were extended to the case of two temperature ions (Gill *et al*. 2006). The case of a charge varying, dusty plasma with a lighter and a heavier ion component was also exhaustively investigated in a series of papers (Pakzad & Javidan 2008; Pakzad 2009a; Pakzad 2009b; Pakzad 2010). Similarly, the case of nonlinear DAWs in a plasma with positive and negative ions (Annou *et al*. 2011) and the effect of dust size distribution was also considered (Annou & Annou 2011). The effect of dust size, mass and charge distribution on DASW in a plasma with electrons (described by a Maxwellian distribution) and nonthermal lighter and heavier ions was also investigated (Moghadam & Dorranian 2013). Only rarefactive solitons were shown to exist. The propagation of DASWs in a collisionless, unmagnetised, cold dusty plasma with electrons and ions modelled by kappa-type distributions was considered by Saini *et al.* (2015); dust acoustic compressive waves were also studied in a warm, dusty plasma containing nonthermal ions and non-isothermal electrons (Dev *et al.* 2015). The more general case of three dimensional solitary waves, in a charge varying dusty plasma, with the electrons and ions obeying a Maxwellian distribution was studied by El-Shorbagy *et al.* (2017). And finally Shahein and Seadawy (2019) carried out a bifurcation analysis of the KP and mKP equations for a unmagnetised, dusty plasma with nonthermal, multi-temperature ions.

Cometary activity starts as it approaches the Sun: the dissociation of water molecules is a source of both oxygen and hydrogen, in addition to solar hydrogen (Brinca & Tsurutani 1987). The other positively charged ions include He^+, He^{2+}, OH^+, C^+, etc. (Balsiger *et al*. 1986; Rubin *et al*. 2009). Thus lighter and heavier ions are an integral part of any cometary plasma. Observations by spacecrafts Vega 1 and Vega 2 provided the first direct measurements of the physical and chemical properties of cometary dust at Halley (Kissel *et al*. 1986). It has also been shown that the sign of the potential on the dust grains, in the tail of comet Halley, varied from − 8V to zero to +7V (Ellis & Neft 1991); thus variation of charges on the dust grains is evident. More recently, the dust equilibrium potential of dust particles observed at Comet 67P/ Churyumov–Gerasimenko was found to vary from − 20V to 0V (Fulle *et al*. 2015). Some of the popular mechanisms suggested for the production of non-Maxwellian distributions, with high energy tails, are the presence of high gradients of particle concentrations or temperatures (Roussel-Dupre 1980), velocity space diffusion due to a supra-thermal radiation field (Hasegawa *et al*. 1985) and wave-particle interactions (Ma & Summers 1988). Theoretically, it has been shown that empirical kappa distributions emerge from statistical mechanics and thermodynamics; from a generalised, statistical mechanics formulated for a collisionless plasma far from a Maxwell-Boltzmann equilibrium but containing turbulence in quasi-stationary equilibrium (Livadiotis & McComas 2010, 2011). And, cometary electrons observed by Rosetta at comet 67P / Churyumov-Gerasimenko were modelled as a superposition of two kappa distribution (Broiles *et al*. 2016).

Thus, for reasons given above we model the cometary plasma as consisting of five components: charge varying dust grains, two components of electrons (modelled by kappa distributions), a lighter (hydrogen) ion component and a heavier (oxygen) ion component. We have derived that Kadomstev–Petiashvili (KP) in three dimensions for the system. For typical parameters observed at comet Halley we find that the system supports rarefactive dust acoustic solitary waves (DASWs) whose amplitudes are larger when the charges on the dust particles are varying. We also find that the amplitudes increase with increasing $z_{d0}n_{d0}$ (product of equilibrium charge number and density of dust) and increasing ion densities. It, however decreases with increasing spectral indices of the electrons.

2. Basic equations

We intend studying dust acoustic solitary waves (DASWs) in a five component, dusty cometary plasma in which the charges on the dust particles are varying. The other components include two components of electrons with different temperatures and characterised by kappa distributions with different spectral indices. The other two species are a lighter, hydrogen ion component and a heavier, oxygen ion component; both modelled by Maxwellian distributions.

The dynamics of the dust particles are governed by the equations of continuity and momentum. The normalised form of these equations are:

$$\frac{\partial n_d}{\partial t} + \vec{\nabla}.(n_d \vec{u}_d) = 0 \tag{1}$$

and

$$\frac{\partial \vec{u}_d}{\partial t} + (\vec{u}_d.\vec{\nabla})\vec{u}_d = Z_d \vec{\nabla}\varphi - \frac{5}{3}\frac{1}{n_d^{1/3}}\vec{\nabla} n_d \tag{2}$$

In Equations (1) and (2), the space ($\vec{x}$) and time (t) variables are normalised, respectively, by the dust Debye length $\lambda_d = \left(\frac{Z_{d0} k_B T_{eff}}{4\pi e^2 Z_{d0}^2 n_{d0}}\right)^{\frac{1}{2}}$ and dust plasma frequency $\omega_{pd} = \left(\frac{4\pi Z_{d0}^2 e^2 n_{d0}}{m_d}\right)^{\frac{1}{2}}$. Here 'e' is the charge, 'k_B' the Boltzmann's constant, while T_{eff} is the effective temperature defined by

$$T_{eff} = \frac{Z_{d0} n_{d0}}{\left[\frac{n_{se0}}{T_{se}} + \frac{n_{ce0}}{T_{ce}} + \frac{n_{li0}}{T_{li}} + \frac{n_{hi0}}{T_{hi}}\right]} \tag{3}$$

In the above, Z_{d0} is the equilibrium charge number on the dust particles; in general n, T and m denote densities, temperatures and masses respectively. The symbols that denote the species are: '*d*' (dust), '*li*' (lighter ions, hydrogen), '*hi*' (heavier ions, oxygen), '*se*' (hotter, solar electrons) and '*ce*' (colder, cometary electrons); '0' denotes equilibrium values.

In Equations (1) and (2), dust density n_d is normalised by n_{d0}, Z_d by Z_{d0}, velocity u_d by $\left(\frac{Z_{d0} k_B T_{eff}}{m_d}\right)^{\frac{1}{2}}$, potential φ by $\frac{k_B T_{eff}}{e}$ while the equation of state for the dust particles is $\frac{p_d}{p_{d0}} = \left(\frac{n_d}{n_{d0}}\right)^{\gamma}$ where $p_{d0} = n_{d0} k_B T_d$ and $\gamma = \frac{5}{3}$ for a 3D case; also $\sigma_d = \frac{T_d}{T_{eff}}\frac{1}{Z_{d0}}$.

The density distributions for the ions (both lighter and heavier ions) are assumed to be Maxwellian and, as mentioned above, the two components of electrons are described by kappa distributions. Thus, their normalised forms are:

$$n_q = \mu_q \exp(-s_q \varphi) \quad q = \text{'}li\text{' or '}hi\text{'} \tag{4}$$

$$n_r = \mu_r \left[1 - \frac{s_r \varphi}{\kappa_r - \frac{3}{2}}\right]^{-\kappa_r + \frac{1}{2}} \quad r = \text{'}se\text{' or '}ce\text{'} \tag{5}$$

In Equations (4) and (5), the densities are normalised by $Z_{d0} n_{d0}$ while on the right side μ_s are defined as

$$\mu_{q(r)} = \frac{n_{q(r),0}}{Z_{d0} n_{d0}} \tag{6}$$

The symbols 's' on the right side are the temperature ratios

$$s_{q(r)} = \frac{T_{eff}}{T_{q(r)}} \tag{7}$$

This set of equations is closed by the Poisson's equation which, in its normalised form, is

$$\nabla^2 \phi = Z_d n_d + \mu_{se}\left(1 - \frac{s_{se}\phi}{\kappa_{se} - \frac{3}{2}}\right)^{-\kappa_{se} + \frac{1}{2}} + \mu_{ce}\left(1 - \frac{s_{ce}\phi}{\kappa_{ce} - \frac{3}{2}}\right)^{-\kappa_{ce} + \frac{1}{2}} - \mu_{li}\exp(-s_{li}\phi) - \mu_{hi}\exp(-s_{hi}\phi) \tag{8}$$

2.1 *Charging currents*

We assume that the dust grains are charged by the electron and ion currents (denoted by I) flowing to the grain's surface. Thus the dust charge variable Q_d is determined by the current balance condition (Xie *et al.* 1998).

$$\frac{\partial Q_d}{\partial t} + (u_d.\nabla)Q_d = I_{se} + I_{ce} + I_{li} + I_{hi} \tag{9}$$

The dust charging time is of the order of 10^{-8} s while the characteristic time for dust motion, for micrometer-sized grains, is $\sim 10^{-3}$ s. The dust charge thus quickly reaches equilibrium, at which point the currents due to electrons and ions are balanced. Thus $\frac{dQ_d}{dt} << 1$, and from Equation (9):

$$I_{se} + I_{ce} + I_{li} + I_{hi} \approx 0 \tag{10}$$

Since we have assumed a Maxwellian distribution for the ions, the corresponding charging currents are (Shukla and Mamun 2002; Pakzad 2009a)

$$I_q = e\pi r_d^2 \left(\frac{8T_q}{\pi m_q}\right)^{\frac{1}{2}} \left(1 - \frac{e\psi}{T_q}\right) n_q \quad q = \text{'}li\text{' or '}hi\text{'} \tag{11}$$

where ψ denotes the dust grain surface potential relative to the plasma potential φ, r_d is the grain radius and the other notations are as defined. The electron currents to the given surface are given by (Abid *et al.* 2013)

$$I_r = -2\sqrt{\pi}r_d^2 B_{\kappa,r}\left(1 - \frac{2e\psi}{\kappa_r m_e \theta_r^2}\right)^{-\kappa_r+1} en_r\theta_r \quad (12)$$

where

$$B_{\kappa,r} = \frac{\kappa_r}{\kappa_r - 1}\left\{\frac{\Gamma(\kappa_r+1)}{\kappa_r^{\frac{3}{2}}\Gamma\left(\kappa_r - \frac{1}{2}\right)}\right\} \quad (13)$$

and

$$\theta_r = \left(\frac{2\kappa_r - 3}{\kappa_r}\right)^{\frac{1}{2}}\left(\frac{T_r}{m_e}\right)^{\frac{1}{2}} \quad \text{r = `}se\text{' or `}ce\text{'} \quad (14)$$

Relation (10) can be used to determine the charges on the dust particles since $Q_d = C\psi$ with $C(= r_d)$ being the capacitance of the dust grain. The normalised dust charge is $Z_d = \frac{\psi}{\psi_0}$ where $\psi_0 = \psi(\varphi = 0)$ is the surface potential on the dust particle with respect to the plasma potential at infinity $(\varphi = 0)$. ψ_0 can be determined from the equilibrium current balance condition (10) as:

$$A_1(1 - s_{li}\psi_0) + A_2(1 - s_{hi}\psi_0) - A_3\left(\frac{2\kappa_{ce} - 3}{2\kappa_{ce}}\right)^{\frac{1}{2}}\left[1 - \frac{s_{ce}\psi_0}{\kappa_{ce} - \frac{3}{2}}\right]^{1-\kappa_{ce}} - A_4\left(\frac{2\kappa_{se} - 3}{2\kappa_{se}}\right)^{\frac{1}{2}}\left[1 - \frac{s_{se}\psi_0}{\kappa_{se} - \frac{3}{2}}\right]^{1-\kappa_{se}} = 0 \quad (15)$$

where

$$A_r = \mu_r\left(\frac{T_r}{T_{ce}}\frac{m_e}{m_r}\right)^{\frac{1}{2}} \quad r = 1, \text{ `}li\text{'}; 2, \text{ `}hi\text{'} \quad (16a)$$

$$A_q = \mu_q B_{\kappa q}\left(\frac{T_q}{T_{ce}}\right)^{\frac{1}{2}} \quad q = 3, \text{ `}ce\text{'}; 4, \text{ `}se\text{'} \quad (16b)$$

3. Derivation of the Kadomstev–Petviashvili (KP) equation

In order to study the dynamics of small amplitude DASWs, in which the charges on the dust particles vary, we use the reductive perturbation technique (Washimi & Taniuti 1966). To apply this method we introduce the stretched variables (El-Labany *et al.* 2004b).

$$X = \varepsilon^{\frac{1}{2}}(x - \lambda t)$$
$$Y = \varepsilon y$$
$$Z = \varepsilon z$$
$$\text{and} \quad T = \varepsilon^{\frac{3}{2}} t \quad (17)$$

where ε is a small parameter indicative of the magnitude of the perturbation and λ is the normalised velocity of the solitary wave. The plasma parameters can be expanded as a power series in ε as

$$n_d = 1 + \varepsilon n_d^{(1)} + \varepsilon^2 n_d^{(2)} \quad (18a)$$

$$u_{dx} = \varepsilon u_{dx}^{(1)} + \varepsilon^2 u_{dx}^{(2)} \quad (18b)$$

$$u_{dy(z)} = \varepsilon^{\frac{3}{2}} u_{dy(z)}^{(1)} + \varepsilon^2 u_{dy(z)}^{(2)} \quad (18c)$$

$$\varphi = \varepsilon\varphi^{(1)} + \varepsilon^2\varphi^{(2)} \quad (18d)$$

$$Z_d = 1 + \varepsilon Z_d^{(1)} + \varepsilon^2 Z_d^{(2)} \quad (18e)$$

with

$$Z_d^{(1)} = \gamma_1\varphi^{(1)} \quad \text{and} \quad Z_d^{(2)} = \gamma_1\varphi^{(2)} + \gamma_2\left(\varphi^{(1)}\right)^2 \quad (18f)$$

and

$$\gamma_1 = \frac{1}{\psi_0}\frac{\partial\psi}{\partial\varphi}\bigg|_{\varphi=0} \quad \text{and} \quad \gamma_2 = \frac{1}{2}\frac{1}{\psi_0}\frac{\partial^2\psi}{\partial\varphi^2}\bigg|_{\varphi=0} \quad (18g)$$

The expressions for γ_1 and γ_2 can be easily got from Equations (10), (11) and (12) and are given in an appendix, namely Appendix 1.

We next proceed to the derivation of the KP equation. Using Equations (8) and (18a) to (18f) in Equations (1) and (2), we get the following relations, to the lowest order in ε:

$$u_{dx}^{(1)} = \lambda n_d^{(1)} = \frac{\lambda}{\Delta}\varphi^{(1)} \quad (19)$$

with

$$\Delta = \frac{5}{3}\sigma_d - \lambda^2 \quad (20)$$

To the next higher order in ε, we get

$$\frac{\partial n_d^{(1)}}{\partial T} - \lambda\frac{\partial n_d^{(2)}}{\partial X} + \frac{\partial}{\partial X}\left(n_d^{(1)}u_{dx}^{(1)} + u_{dx}^{(2)}\right) + \frac{\partial}{\partial Y}u_{dy}^{(1)} + \frac{\partial}{\partial Z}u_{dz}^{(1)} = 0 \quad (21a)$$

$$\frac{\partial u_{dx}^{(1)}}{\partial T} - \lambda \frac{\partial u_{dx}^{(2)}}{\partial X} + u_{dx}^{(1)} \frac{\partial}{\partial X} u_{dx}^{(1)} - Z_d^{(1)} \frac{\partial \varphi^{(1)}}{\partial X} - \frac{\partial \varphi^{(2)}}{\partial X} + \frac{5}{3}\sigma_d \frac{\partial n_d^{(2)}}{\partial X} - \frac{5}{9}\sigma_d n_d^{(1)} \frac{\partial n_d^{(1)}}{\partial X} = 0 \tag{21b}$$

$$\frac{\partial}{\partial Y}\left(\frac{\partial}{\partial X} u_{dy}^{(1)}\right) = \frac{\lambda}{\Delta}\frac{\partial^2 \varphi^{(1)}}{\partial Y^2} \tag{21c}$$

$$\frac{\partial}{\partial Z}\left(\frac{\partial}{\partial X} u_{dz}^{(1)}\right) = \frac{\lambda}{\Delta}\frac{\partial^2 \varphi^{(1)}}{\partial Z^2} \tag{21d}$$

And from Poisson's equation (3) we get, to order ε,

$$\lambda^2 = \frac{5}{3}\sigma_d + (\gamma_1 + T')^{-1} \tag{22}$$

where

$$T' = \mu_{se} s_{se} \frac{2\kappa_{se} - 1}{2\kappa_{se} - 3} + \mu_{ce} s_{ce} \frac{2\kappa_{ce} - 1}{2\kappa_{ce} - 3} + \mu_{li} s_{li} + \mu_{hi} s_{hi} \tag{23}$$

As a check on Equation (23), we note that $T' = 1$ as the spectral indices $\kappa_{se}, \kappa_{ce} \to \infty$ and we neglect one electron and one ion component (say '*ce*' and '*hi*') and thus Equation (22) reduces to the corresponding expression for λ^2 in (El-Labany *et al.* 2004b). At this juncture, a few remarks regarding λ are in order. For the special case of an electron depleted plasma ($n_{se} = n_{ce} = 0$) and with $T_{li} = T_{hi} = T_i$ we find that $T_{eff} = T_i$. Substituting into Equation (22), we find that λ (no dust charge variation) > λ (dust charge varies). A similar result can also be arrived at if $T_{se}, T_{ce} >> T_{hi}, T_{li}$. And in both the cases λ is directly proportional to T_d, the dust temperature and inversely proportional to z_{do}, the equilibrium charge on the dust grains. Also, if in addition to the above requirements, $T_d = 0$, λ is a constant.

And equating terms of coefficients of order ε^2, we get

$$\frac{\partial^2 \varphi^{(1)}}{\partial X^2} = Z_d^{(1)} n_d^{(1)} + n_d^{(2)} + Z_d^{(2)} + \mu_{se}\left[\frac{2\kappa_{se} - 1}{2\kappa_{se} - 3} s_{se}\varphi^{(2)} + \frac{(2\kappa_{se} - 1)(2\kappa_{se} + 1)}{2(2\kappa_{se} - 3)^2} s_{se}^2 \left(\varphi^{(1)}\right)^2\right] + \mu_{ce}\left[\frac{2\kappa_{ce} - 1}{2\kappa_{ce} - 3} s_{ce}\varphi^{(2)} + \frac{(2\kappa_{ce} - 1)(2\kappa_{ce} + 1)}{2(2\kappa_{ce} - 3)^2} s_{ce}^2 \left(\varphi^{(1)}\right)^2\right] - \mu_{li}\left[1 - s_{li}\varphi^{(2)} + \frac{s_{li}^2}{2}\left(\varphi^{(1)}\right)^2\right] - \mu_{hi}\left[1 - s_{hi}\varphi^{(2)} + \frac{s_{hi}^2}{2}\left(\varphi^{(1)}\right)^2\right] \tag{24}$$

Using Equations (18f) and (19)–(23) in conjunction with Equation (24), we can finally arrive at the Kadomstev–Petviashvili equation as

$$\frac{\partial}{\partial X}\left\{\frac{\partial \varphi^{(1)}}{\partial T} + \frac{A}{2}\frac{\partial^3 \varphi^{(1)}}{\partial X^3} + AB\varphi^{(1)}\frac{\partial \varphi^{(1)}}{\partial X}\right\} + D\left\{\frac{\partial^2 \varphi^{(1)}}{\partial Y^2} + \frac{\partial^2 \varphi^{(1)}}{\partial Z^2}\right\} = 0 \tag{25}$$

where

$$A = \frac{\Delta^2}{\lambda} \tag{26a}$$

$$B = \frac{1}{2}\left[\frac{3\lambda^2 - \frac{5}{9}\sigma_d}{\Delta^3} - \frac{3\gamma_1}{\Delta} - 2\gamma_2 - Q\right] \tag{26b}$$

$$D = \frac{\lambda}{2} \tag{26c}$$

with

$$Q = \mu_{se} s_{se}^2 \frac{(2\kappa_{se} - 1)(2\kappa_{se} + 1)}{(2\kappa_{se} - 3)^2} + \mu_{ce} s_{ce}^2 \frac{(2\kappa_{ce} - 1)(2\kappa_{ce} + 1)}{(2\kappa_{ce} - 3)^2} - \mu_{li} s_{li}^2 - \mu_{hi} s_{hi}^2 \tag{27}$$

Again, if we neglect one electron and one ion component ('*ce*' and '*hi*'), we can show that Q reduces to the corresponding expression in El-Labany *et al.* (2004b) as $\kappa_{se} \to \infty$.

4. Solution and stability

To solve the KP equation (25), we introduce a new variable (El-Labany *et al.* 2004b)

$$\eta = lX + mY + nZ - UT \tag{28}$$

where l, m and n are the direction cosines of the wave vector along the X, Y and Z axes. Also, $l^2 + m^2 + n^2 = 1$. Integrating Equation (25), with respect to η and using the boundary conditions that $\varphi^{(1)}$ and $\frac{\partial \varphi^{(1)}}{\partial \eta} \to 0$ as $\eta \to \infty$, we get

$$\frac{\partial^2 \varphi^{(1)}}{\partial \eta^2} = \frac{2h}{Al^4} \varphi^{(1)} - \frac{B}{l^2} \left(\varphi^{(1)}\right)^2 \quad (29)$$

The one soliton solution of Equation (29) is given by

$$\varphi^{(1)} = \varphi_0 \sec h^2 \left(\frac{\eta}{\omega}\right) \quad (30)$$

where φ_0 is the amplitude of the solitary wave and ω, its width. The expressions for the amplitude and width are:

$$\varphi_0 = \frac{3h}{ABl^2} \quad (31)$$

$$\omega = \frac{1}{\sqrt{\frac{2h}{Al^4}}} \quad (32)$$

with $h = Ul - D(1 - l^2)$.

5. Discussion

The KP equation (25) derived by us is a generalisation of many such equations derived earlier. For example, the equation was derived in a three component dusty plasma by El-Labany *et al.* (2004b). Similarly, the equation was studied in a four component dusty plasma (Pakzad 2009a, b). Also, the Kadomstev–Petviashvili–Burger's (KPB) equation was studied in a five component plasma with two components of electrons, one component of lighter ions and a pair of oppositely charged heavier ions (Manesh *et al.* 2015). Thus the present study, which considers charge variations on the dust particles, can be considered complementary to this study and generalisations of the other studies mentioned above.

Finally, a perusal of the KP equation (25) reveals that while all the coefficients are implicitly affected by the parameters of the plasma, it is the nonlinear coefficient B that shows an explicit dependence on the extra constituent's density and temperature.

6. Results

A popular model of a comet, substantiated by observations, is that of an atmosphere of hydrogen, water molecules and dust particles. The dissociation of the molecules of water results in the release of hydrogen and oxygen ions; in our study both these ions have been modelled by Maxwellian distributions. The observed value of the hydrogen density was $n_H = 4.95$ cm^{-3}, at a temperature of $T_H = 8 \times 10^4$ K (Brinca & Tsurutani 1987). The temperature of the second colder component of electrons was set at 2×10^4 K. And to conform to recent experimental observations, both components of electrons were modelled by kappa distributions (Broiles *et al.* 2016). The heavier, oxygen ion density was $n_{o^+} = 0.5$ cm^{-3}, at a temperature of 1.16×10^4 K (Brinca & Tsurutani 1987); the temperature of the dust was also assumed to be the same. Also, the equilibrium dust density was set at 0.005 cm^{-3} and the equilibrium charge number = 200 giving a product of $z_{d0} n_{d0} = 1.0$.

Figure 1 is a plot of the DASW amplitude, the parameters for the figure being densities n_{li0} = 4.95 cm^{-3}, n_{hi0} = 0.5 cm^{-3} and n_{d0} = 0.005 cm^{-3}, temperatures T_{se} = 2 × 10^5 K, T_{ce} = 2 × 10^4 K, T_{li} = 8 × 10^4 K, T_{hi} = 2.8 × 10^4 K and T_d = 1.16 × 10^4 K, charge numbers z_{hi} = 1, z_{li} = 1 and z_{d0} = 200, spectral indices κ_{se} = 2 and κ_{ce} = 2, U = 0.1 and l = 0.9. Curve (a) is when the case where the dust charges on the grain surface are a constant while curve (b) is when the charges vary. We find that while the DASW is rarefactive in nature, the amplitude of the solitary wave is larger when the charges on the dust surface vary.

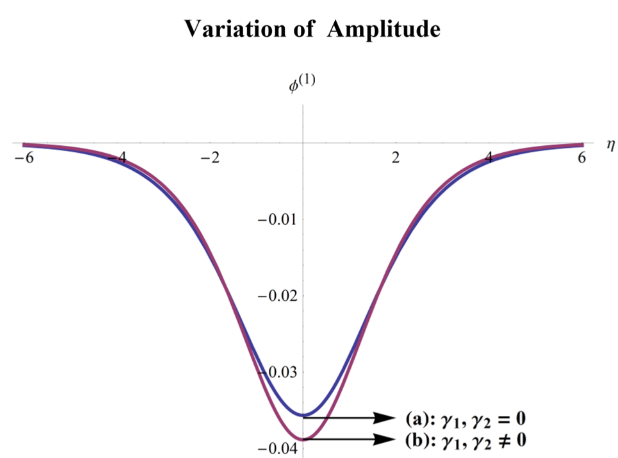

Figure 1. Variation of DASW amplitude. The other parameters are: $n_{d0} = 0.005$ cm^{-3}, $n_{hi0} = 0.5$ cm^{-3}, $n_{li0} = 4.95$ cm^{-3}, $\kappa_{se} = 2$, $\kappa_{ce} = 2$, $U = 0.1$, $l = 0.9$, $m_{li} = 1.67 \times 10^{-24}$g, $m_{hi} = 16 \times 1.67 \times 10^{-24}$ g, $m_e = 9.1 \times 10^{-28}$g, $z_{d0} = 200$, $z_{hi} = 1$, $z_{li} = 1$, $T_{ce} = 2 \times 10^4$K, $T_d = 1.16 \times 10^4$K, $T_{se} = 2 \times 10^5$ K, $T_{li} = 8 \times 10^4$ K, $T_{hi} = 2.8 \times 10^4$ K.

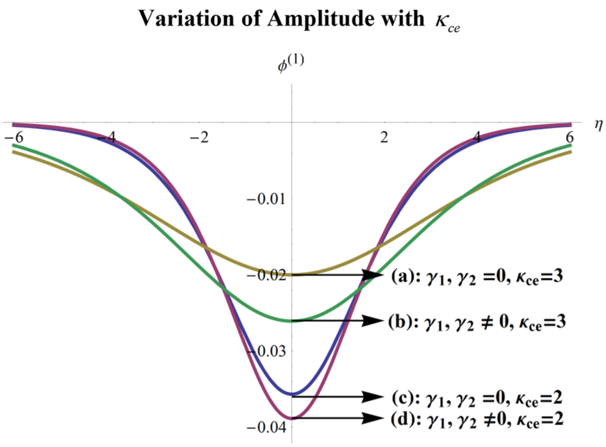

Figure 2. Variation of Amplitude with κ_{ce}. The other parameters are: $n_{d0} = 0.005$ cm^{-3}, $n_{hi0} = 0.5$ cm^{-3}, $n_{li0} = 4.95$ cm^{-3}, $\kappa_{se} = 2$, $U = 0.1, l = 0.9$, $z_{li} = 1$, $z_{d0} = 200$, $z_{hi} = 1$, $m_{li} = 1.67 \times 10^{-24}$g, $m_{hi} = 16 \times .67 \times 10^{-24}$ g, ;$m_e = 9.1 \times 10^{-28}$g, $T_{ce} = 2 \times 10^4$K, $T_d = 1.16 \times 10^4$K, $T_{se} = 2 \times 10^5$ K, $T_{li} = 8 \times 10^4$ K, $T_{hi} = 2.8 \times 10^4$ K.

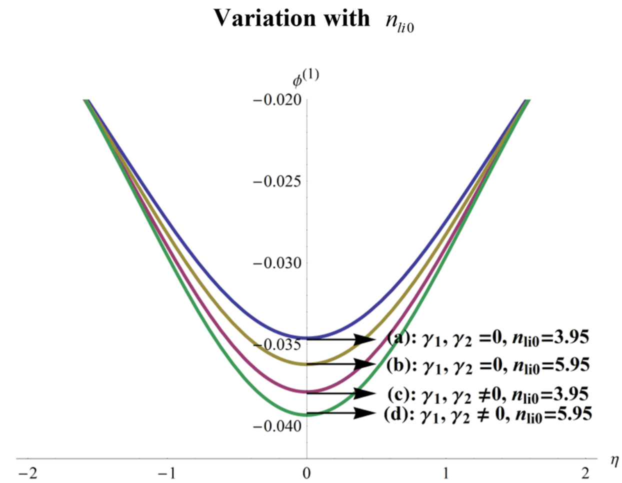

Figure 3. Variation with n_{li0}. The other parameters are: $n_{d0} = 0.005$ cm^{-3}, $n_{hi0} = 0.5$ cm^{-3}, $\kappa_{se} = 2$, $\kappa_{ce} = 2$, $U = 0.1$, $l = 0.9$, $z_{li} = 1$, $z_{d0} = 200$, $z_{hi} = 1$, $m_{li} = 1.67 \times 10^{-24}$ g, $m_{hi} = 16 \times 1.67 \times 10^{-24}$ g, $m_e = 9.1 \times 10^{-28}$g, $T_{ce} = 2 \times 10^4$ K, $T_d = 1.16 \times 10^4$ K, $T_{se} = 2 \times 0^5$ K, $T_{li} = 8 \times 10^4$ K, $T_{hi} = 2.8 \times 10^4$ K.

The amplitude of the DASW as a function of κ_{ce}, the spectral index of the second component of electrons is studied next. Figure 2 depicts the amplitude of the DASW, for two values of κ_{ce}, for the case of a constant and varying potential on the grain surface. Curve (a) is for the case of $\kappa_{ce} = 3$ (constant charge), while curve (b) is for varying charge on the grain's surface. The corresponding curves for $\kappa_{ce} = 2$ are depicted respectively by (c) and (d). We find that the amplitude is appreciably larger for $\kappa_{ce} = 2$ as compared to $\kappa_{ce} = 3$; also, as in Figure 1, the amplitudes are larger when the charges on the grain's surface vary.

Figure 3 depicts the variation of the amplitude of the DASW for two values of the lighter ion hydrogen density. Curve (a) is for $n_{li0} = 3.95$ cm^{-3} and curve (b) is for $n_{li0} = 5.95$ cm^{-3}, both for the cases where the charges on the dust grains are a constant. The other parameters for the figure are densities $n_{hi0} = 0.5$ cm^{-3} and $n_{d0} = 0.005$ cm^{-3}, temperatures $T_{se} = 2 \times 10^5$ K, $T_{ce} = 2 \times 10^4$ K, $T_{li} = 8 \times 10^4$ K, $T_{hi} = 2.8 \times 10^4$ K and $T_d = 1.16 \times 10^4$ K, charge numbers $z_{hi} = 1$, $z_{li} = 1$ and $z_{d0} = 200$, spectral indices $\kappa_{se} = 2$ and $\kappa_{ce} = 2$, $U = 0.1$ and $l = 0.9$. Similarly, curves (c) and (d) correspond to the case where the charges on the dust grains vary. As in previous cases, the amplitudes are larger when the charges are varying; however, the amplitudes are also larger when the densities of the lighter ions increase. A similar result is also seen when there is an increase in the heavier ion density oxygen. Since one of the sources of these ions is the dissociation of water molecules, the amplitudes of the DASWs are likely to increase as the comet approaches the Sun.

Figure 4 is a plot of the amplitude of the DASW for two values of the product $z_{d0}n_{d0}$; the other parameters for the figure being densities $n_{li0} = 4.95$ cm^{-3} and $n_{hi0} = 0.5$ cm^{-3}, temperatures $T_{se} = 2 \times 10^5$ K, $T_{ce} = 2 \times 10^4$ K, $T_{li} = 8 \times 10^4$ K, $T_{hi} = 2.8 \times 10^4$ K and $T_d = 1.16 \times 10^4$ K, charge numbers $z_{hi} = 1$ and $z_{li} = 1$, spectral indices $\kappa_{se} = 2$ and $\kappa_{ce} = 2$, $U = 0.1$ and $l = 0.9$. Curves (a) and (c) are respectively for $z_{d0}n_{d0} = 0.5$ and 1 (no variation of charge on the dust grains) while curves (b) and (d) are for the case when the charges are varying. Again the amplitudes increase when the dust charge is varying; also the amplitude increases with increasing $z_{d0}n_{d0}$.

We are considering the case where both electrons and ions contribute to the variation of charges on the dust grains. Assimilation of the ions and electrons would lead to an increase in the kinetic energy of the dust grains and a consequent increase in the amplitude of the oscillations. A kappa distribution tends to a Maxwellian distribution when the spectral index $\kappa \to \infty$. Hence, as κ decreases the proportion of superthermal particles increase and consequently the amount of energy deposited on the grains. Thus again the amplitude of oscillation increases. Similarly, increasing ion densities would lead to an increase of charge neutralisation of the charges on the dust grains. This, in turn, would allow more

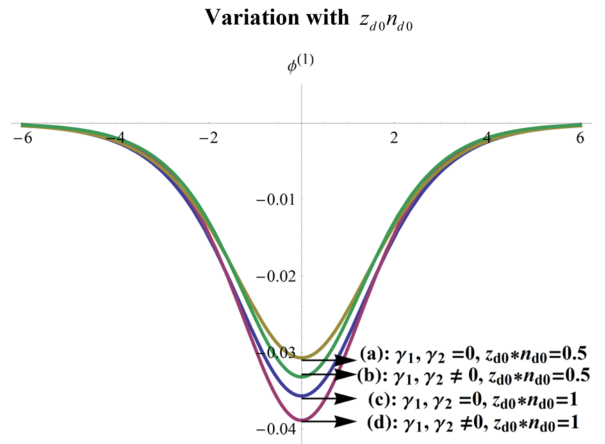

Figure 4. Variation with $z_{d0}n_{d0}$. The other parameters are: $n_{hi0} = 0.5$ cm^{-3}, $n_{li0} = 4.95$ cm^{-3}, $\kappa_{se} = 2$, $\kappa_{ce} = 2$, $U = 0.1$, $l = 0.9$, $z_{hi} = 1$, $z_{li} = 1$, $m_{li} = 1.67 \times 10^{-24}$g, $m_{hi} = 16 \times 1.67 \times 10^{-24}$ g, $m_e = 9.1 \times 10^{-28}$ g, $T_{ce} = 2 \times 10^4$ K, $T_d = 1.16 \times 10^4$ K, $T_{se} = 2 \times 10^5$ K, $T_{li} = 8 \times 10^4$ K, $T_{hi} = 2.8 \times 10^4$ K.

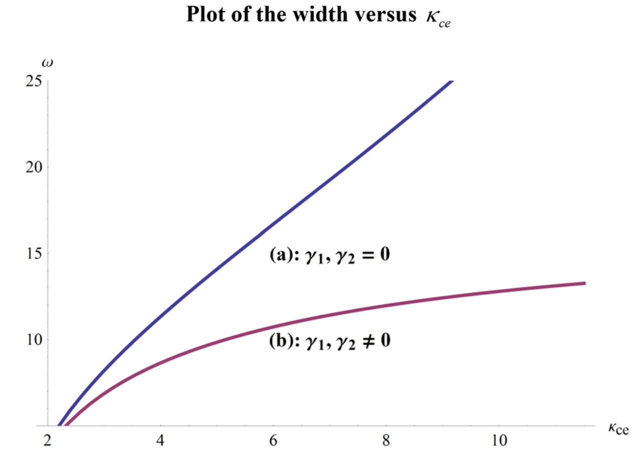

Figure 5. Plot of the width versus κ_{ce}. The other parameters are: $n_{d0} = 0.005$ cm^{-3}, $n_{hi0} = 0.5$ cm^{-3}, $n_{li0} = 4.95$ cm^{-3}, $\kappa_{se} = 2$, $U = 0.1$, $l = 0.9$, $z_{li} = 1$, $z_{d0} = 200$, $z_{hi} = 1$, $m_{li} = 1.67 \times 10^{-24}$g, $m_{hi} = 16 \times 1.67 \times 10^{-24}$ g, $m_e = 9.1 \times 10^{-28}$g, $T_{ce} = 2 \times 10^4$K, $T_d = 1.16 \times 10^4$K, $T_{se} = 2 \times 10^5$K, $T_{li} = 8 \times 10^4$ K, $T_{hi} = 2.8 \times 10^4$ K.

superthermal electrons to reach the grains' surfaces. Thus, both ions and electrons could contribute to an increase in the amplitude when the ion density increases. Finally, an increasing $z_{d0}n_{d0}$ would attract more ions leading to an increase in amplitude as pictured above.

Figure 5 is a plot of the width ω versus the spectral index κ_{ce} of the cometary electrons; the other parameters for the figure are: densities $n_{li0} = 4.95$ cm^{-3}, $n_{hi0} = 0.5$ cm^{-3} and $n_{d0} = 0.005$ cm^{-3}, temperatures $T_{se} = 2 \times 10^5$ K, $T_{ce} = 2 \times 10^4$ K, $T_{li} = 8 \times 10^4$ K, $T_{hi} = 2.8 \times 10^4$ K and $T_d = 1.16 \times 10^4$ K, charge numbers $z_{hi} = 1$, $z_{li} = 1$ and $z_{d0} = 200$, spectral index $\kappa_{se} = 2$, $U = 0.1$ and $l = 0.9$. Curve (a) is for $\gamma_1 = \gamma_2 = 0$ (that is, the charges on the dust particles are a constant), while curve (b) is for the case where the charges on the dust particles vary ($\gamma_1 \neq 0$, $\gamma_2 \neq 0$). We find that the width of the solitary wave is smaller for the latter case; that is, the solitary waves are more "spiky" when the charges on the dust particles vary (Tribeche & Bacha 2010).

Figure 6 too depicts the variation of the width of the solitary wave but as a function of the density of the lighter ions. The parameters for the figure are: densities $n_{hi0} = 0.5$ cm^{-3} and $n_{d0} = 0.005$ cm^{-3}, temperatures $T_{se} = 2 \times 10^5$ K, $T_{ce} = 2 \times 10^4$ K, $T_{li} = 8 \times 10^4$ K, $T_{hi} = 2.8 \times 10^4$ K and $T_d = 1.16 \times 10^4$ K, charge numbers $z_{hi} = 1$, $z_{li} = 1$ and $z_{d0} = 200$, spectral indices $\kappa_{se} = 2$ and $\kappa_{ce} = 2$, $U = 0.1$ and $l = 0.9$. Again curve (a) is for the case

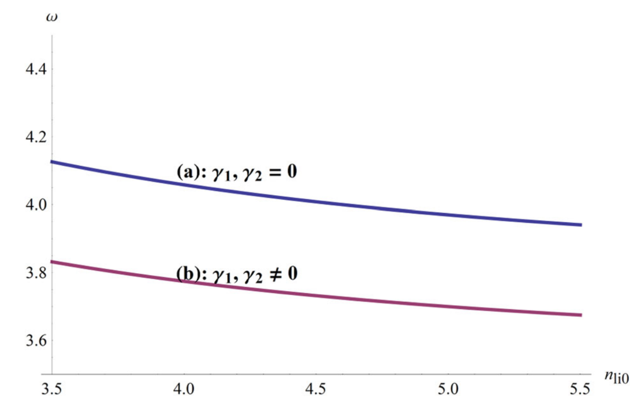

Figure 6. Plot of the width versus n_{li0}. The other parameters are: $n_{d0} = 0.005$ cm^{-3}, $n_{hi0} = 0.5$ cm^{-3}, $\kappa_{se} = 2$, $\kappa_{ce} = 2$, $U = 0.1$, $l = 0.9$, $z_{li} = 1$, $z_{d0} = 200$, $z_{hi} = 1$, $m_{li} = 1.67 \times 10^{-24}$g, $m_{hi} = 16 \times 1.67 \times 10^{-24}$g, $m_e = 9.1 \times 10^{-28}$g, $T_{ce} = 2 \times 10^4$K, $T_d = 1.16 \times 10^4$K, $T_{se} = 2 \times 10^5$ K, $T_{li} = 8 \times 10^4$ K, $T_{hi} = 2.8 \times 10^4$ K.

where the charges on the dust particles are a constant ($\gamma_1 = \gamma_2 = 0$); curve (b) is for the situation where the charges on the dust particles vary ($\gamma_1 \neq 0$, $\gamma_2 \neq 0$). The width is again smaller when the charges on the dust particles are not a constant. The variation of the width of the solitary waves as a function of n_{hi0}, the equilibrium density of the heavier ions is very similar to the above variation with respect to the lighter ions.

Vega observations of comet Halley had found two internal boundaries at approximately 770,000 and 350,000 km from the nucleus. Important signatures observed at these boundaries along with Giotto observations have been interpreted in terms of giant rarefaction wave and a weak shock wave with solitary waves being generated at the inner edge of the rarefaction wave as well as the shock front (Oberc *et al.* 1989).

The steepening of a nonlinear dust acoustic wave results in a DA shock wave and these nonlinear structures have been observed at all comets. Dissipative features like collisions between dust particles and ions and the fluctuating charges on the dust grains would ultimately lead to the formation of DA shock waves at comets (Naeem *et al.* 2020). In an earlier study (and again applicable to comets) Tribeche and Bacha (2013) concluded that dust charge variation induced nonlinear damping leads to the development of collisionless DA shock waves. Similarly, the pickup of heavy ions (oxygen in our case) could also contribute to the formation of a cometary bow shock (Coates 1995, 2009). In a detailed numerical study, Omidi and Winske (1986) concluded that the macroscopic structure of a quasi-perpendicular shock at comet Halley is determined by the O^+ ions at that distance. Again, in a study of ion acoustic shock waves in a multi-ion plasma applicable to comet Halley, Manesh *et al.* (2016) studied these waves by deriving the Korteweg-deVries-Burgers (KdVB) equation. They found that the ion acoustic solitary wave could make a transition to a shock wave whose strength increased with decreasing spectral indices of the electrons and increasing densities of the positively charged oxygen ion densities.

Thus as mentioned above, the dust acoustic solitary wave could also make a transition to a shock wave since, in addition to electron spectral indices and oxygen ion densities, we also have an additional dissipation mechanism namely varying charges of the dust grains; self-excited DA shocks too have been observed in the laboratory (Heinrich *et al.* 2009). It may also be noted that we have found the amplitude of the DA solitary wave to be smallest in a 3 component plasma (dust, ions and electrons) and largest in our five component plasma thus substantiating the above observations of Tribeche and Bacha (2013) and Coates (1995, 2009). It is intermediate in a four component plasma made up of dust, lighter and heavier ions and electrons; thus the second component of superthermal electrons increases the amplitude of the DA solitary waves. However demonstration of this transition, from a solitary wave to a shock wave, is beyond the scope of this paper.

7. Conclusions

We have, in this paper, studied the characteristics of DASWs in a five component plasma relevant to a comet's environment. The five components include two components of electrons, lighter (hydrogen) ions, heavier (oxygen) ions and negatively charged dust with varying charge on its surface. Guided by recent observations of comet 67P/Churyumov-Gerasimenko we model the two components of electrons by kappa distributions, while both types of ions are described by Maxwellian distributions. We find that the plasma can support rarefactive dust acoustic solitary waves whose amplitude is larger when the charges on the dust particles vary; this amplitude is also larger in the presence of superthermal electrons. Also, the amplitude increases with increasing ion densities. On the other hand, the DASW is narrower when the charges on the dust particles vary and with increasing ion densities. Since dissociation of water molecules is a source of both hydrogen and oxygen ions, we tentatively conclude that small amplitude and narrow rarefactive solitary waves are likely to form as a comet approaches the Sun. And finally, observations at comet Halley have been interpreted in terms of a giant rarefaction wave with solitary waves being generated at the inner edges of this rarefaction wave.

Acknowledgements

The authors thank the reviewer for the insightful comments which have improved the scientific content of the paper.

Appendix 1

The expression for γ_1 and γ_2, which are intimately connected to the charge variation on the dust particles are given in this Appendix.

Expression (15) can be used to calculate ψ_0, the potential on the dust particle when the plasma potential $\varphi = 0$. The first and the second derivative of (10) with the expressions for the currents (11) and (12) substituted results in the formula for γ_1 and γ_2 given in (18g). γ_1, in its final simplified form, can be written as:

$$\gamma_1 = \frac{-1}{\psi_0} \frac{\gamma_b}{\gamma_a} \qquad (\mathrm{A}-1)$$

where

$$\gamma_a = A_1 + A_2\beta + A_3\beta_{1ce}\left(\frac{\kappa_{ce}-\frac{3}{2}}{\kappa_{ce}}\right)^{\frac{1}{2}}\left(\frac{\kappa_{ce}-1}{\kappa_{ce}-\frac{3}{2}}\right)\left(1-\frac{\beta_{1ce}s\psi_0}{\kappa_{ce}-\frac{3}{2}}\right)^{-\kappa_{ce}} + A_4\beta_{1se}\left(\frac{\kappa_{se}-\frac{3}{2}}{\kappa_{se}}\right)^{\frac{1}{2}}\left(\frac{\kappa_{se}-1}{\kappa_{se}-\frac{3}{2}}\right)\left(1-\frac{\beta_{1se}s\psi_0}{\kappa_{se}-\frac{3}{2}}\right)^{-\kappa_{se}} \quad (\mathrm{A}-2)$$

$$\gamma_b = A_1(1-s\psi_0) + A_2\beta(1-\beta s\psi_0) + A_3\beta_{1ce}\left(\frac{\kappa_{ce}-\frac{3}{2}}{\kappa_{ce}}\right)^{\frac{1}{2}}\left(\frac{\kappa_{ce}-\frac{1}{2}}{\kappa_{ce}-\frac{3}{2}}\right)\left(1-\frac{\beta_{1ce}s\psi_0}{\kappa_{ce}-\frac{3}{2}}\right)^{-\kappa_{ce}+1} + A_4\beta_{1se}\left(\frac{\kappa_{se}-\frac{3}{2}}{\kappa_{se}}\right)^{\frac{1}{2}}\left(\frac{\kappa_{se}-\frac{1}{2}}{\kappa_{se}-\frac{3}{2}}\right)\left(1-\frac{\beta_{1se}s\psi_0}{\kappa_{se}-\frac{3}{2}}\right)^{-\kappa_{se}+1} \quad (\mathrm{A}-3)$$

where $s = s_{li}$, $\beta = \frac{s_{hi}}{s}$, $\beta_{1ce} = \frac{s_{ce}}{s}$ and $\beta_{1se} = \frac{s_{se}}{s}$. Also

$$Z_d^{(1)} = \gamma_1\varphi^{(1)} \quad (\mathrm{A}-4)$$

Similarly, the final simplified expression, for γ_2 can be written as

$$\gamma_2 = \frac{1}{2\psi_0}\frac{s(\gamma_{c1}+\gamma_{c2}+\gamma_{c3})}{\gamma_a} \quad (\mathrm{A}-5)$$

with

$$\gamma_{c1} = A_1(1-s\psi_0) + A_2\beta^2(1-\beta s\psi_0) - A_3\beta_{1ce}^2\left(\frac{\kappa_{ce}-\frac{3}{2}}{\kappa_{ce}}\right)^{\frac{1}{2}}\left(\frac{\left(\kappa_{ce}-\frac{1}{2}\right)\left(\kappa_{ce}+\frac{1}{2}\right)}{\left(\kappa_{ce}-\frac{3}{2}\right)^2}\right)\left(1-\frac{\beta_{1ce}s\psi_0}{\kappa_{ce}-\frac{3}{2}}\right)^{-\kappa_{ce}+1} - A_4\beta_{1se}^2\left(\frac{\kappa_{se}-\frac{3}{2}}{\kappa_{se}}\right)^{\frac{1}{2}}\left(\frac{\left(\kappa_{se}-\frac{1}{2}\right)\left(\kappa_{se}+\frac{1}{2}\right)}{\left(\kappa_{se}-\frac{3}{2}\right)^2}\right)\left(1-\frac{\beta_{1se}s\psi_0}{\kappa_{se}-\frac{3}{2}}\right)^{-\kappa_{se}+1} \quad (\mathrm{A}-6)$$

$$\gamma_{c2} = 2\gamma_1\psi_0\left[\begin{array}{c} A_1 + A_2\beta^2 - A_3\beta_{1ce}^2\left(\frac{\kappa_{ce}-\frac{3}{2}}{\kappa_{ce}}\right)^{\frac{1}{2}}\left(\frac{\left(\kappa_{ce}-\frac{1}{2}\right)(\kappa_{ce}-1)}{\left(\kappa_{ce}-\frac{3}{2}\right)^2}\right)\left(1-\frac{\beta_{1ce}s\psi_0}{\kappa_{ce}-\frac{3}{2}}\right)^{-\kappa_{ce}} \\ - A_4\beta_{1se}^2\left(\frac{\kappa_{se}-\frac{3}{2}}{\kappa_{se}}\right)^{\frac{1}{2}}\left(\frac{\left(\kappa_{se}-\frac{1}{2}\right)(\kappa_{se}-1)}{\left(\kappa_{se}-\frac{3}{2}\right)^2}\right)\left(1-\frac{\beta_{1se}s\psi_0}{\kappa_{se}-\frac{3}{2}}\right)^{-\kappa_{se}} \end{array}\right] \quad (\mathrm{A}-7)$$

$$\gamma_{c3} = -(\gamma_1\psi_0)^2\left[\begin{array}{c} A_3\beta_{1ce}^2\left(\frac{\kappa_{ce}-\frac{3}{2}}{\kappa_{ce}}\right)^{\frac{1}{2}}\left(\frac{\kappa_{ce}(\kappa_{ce}-1)}{\left(\kappa_{ce}-\frac{3}{2}\right)^2}\right)\left(1-\frac{\beta_{1ce}s\psi_0}{\kappa_{ce}-\frac{3}{2}}\right)^{-\kappa_{ce}-1} \\ + A_4\beta_{1se}^2\left(\frac{\kappa_{se}-\frac{3}{2}}{\kappa_{se}}\right)^{\frac{1}{2}}\left(\frac{\kappa_{se}(\kappa_{se}-1)}{\left(\kappa_{se}-\frac{3}{2}\right)^2}\right)\left(1-\frac{\beta_{1se}s\psi_0}{\kappa_{se}-\frac{3}{2}}\right)^{-\kappa_{se}-1} \end{array}\right] \quad (\mathrm{A}-8)$$

and $Z_d^{(2)}$, the second-order change in the dust charge is

$$Z_d^{(2)} = \gamma_1 \varphi^{(2)} + \gamma_2 \left(\varphi^{(1)} \right)^2 \qquad (A-9)$$

References

Abid A. A., Ali S., Muhammad R. J. 2013, J. Plasma Phys, 79, 1117

Annou, K., Annou, R. 2011, Plasma Physics P4.039

Annou K., Bahamida S., Annou R. 2011, Pramana, 76, 513

Balsiger H., Altwegg K., Buhler F., Geiss J., Ghielmetti A. G., Goldstein B. E., Goldstein R., Huntress W. T., Ip W. H., Lazarus A. J., Meier A., Neugebauer M., Rettenmund U., Rosenbauer H., Schwenn R., Sharp R. D., Shelley E. G., Ungstrup E., Young D. T. 1986, Nature, 321, 330

Bhatt J. R., Pandey B. P. 1994, Phys. Rev. E, 50, 3980

Brinca A. L., Tsurutani B. T. 1987, Astron. Astrophys., 187, 311

Broiles T. W., Livadiotis G., Burch J. L., Chae K., Clark G., Cravens T. E., Davidson R., Eriksson A., Frahm R. A., Fuselier S. A., Goldstein J., Goldstein R., Henri P., Madanian H., Mandt K., Mokashi P., Pollock C., Rahmati A., Samara M., Schwartz S. J. 2016, J. Geophys. Res., 121, 7407-7422

Coates A. J., 1995, Adv. Space. Res., 15, 403

Coates A. J., 2009, AIP Conf. Proc., 1183, 121

Chu J. H., Du J. B., Lin I. 1994, Appl. Phys., 27, 296

D'Angelo N. 1995, J. Phys D: Appl. Phys., 28, 1009

D' Angelo N., Merlino R.L. 1996, Planet. Sp. Sci., 44, 1593

Dev A. N., Deka M. K., Subedi R., Sarma J. 2015, Plasma Sci. Tech., 17, 721

Duan W. S. 2002, Chaos, Solitons and Fractals, 14, 1315

Duan W. S. 2004, Chinese Phys. B, 13, 598

El-Labany S. K., El-Taibany W. F., Mamun A. A., Moslem W. M. 2004a, Phys. Plasmas, 11, 926

El-Labany S. K., Moslem W. M., El-Taibany W. F., Mahmoud M. 2004b, Phys. Scr., 70, 317.

Ellis T. A., Neft J. S. 1991, Icarus, 91, 280

El-Shorbagy K. H., Mahassen H., El-Bendary A. A. 2017, J. Astrophys. Astr., 38, 69

Fulle M., Corte V. D., Rotundi A., Weissman P., Juhasz A., Szego K., Sordini R., Ferrari M., Ivanovski S., Lucarelli F. 2015, The Astrophys. J. Lett., 802, L12

Gill T. S., Saini N.S., Kaur H. 2006, Chaos, Solitons and Fractals, 28, 1106

Heinrich J., Kim S.-H., Merlino R. L., 2009, Phys. Rev. Lett., 103, 115002

Hasegawa A., Mima K., Duong-van M. 1985, Phys. Rev. Lett., 25, 4099

Jana M.R., Sen A., Kaw P.K. 1993, Phys. Rev. E., 48, 3930

Kadomstev B. B., Petviashvili V. I. 1970, Sov. Phys., 15, 539

Kissel J., Brownlee D. E., Buchler K., Clark B. C., Fechtig H., Grun E., Hornung K., Igenbergs E. B., Jessberger E. K., Krueger F. R., Kuczera H., McDonnell J. A. M., Morfill G. M., Rahe J., Schwehm G. H., Sekanina Z., Utterback N. G., Volk H. J., Zook H. A. 1986, Nature, 321, 336

Lakshmi S. V., Bharuthram R., Rao N.N., Shukla P.K. 1997, Planet. Sp. Sci., 45, 355

Livadiotis G., McComas D. J., 2010, Astrophys. J., 714, 971

Livadiotis G., McComas D. J., 2011, Astrophys. J., 744, 88

Ma C.-Y., Summers D. 1988, Geophys. Res. Lett., 25, 4099

Mamun A. A. 1998, Phys. Scr., 58, 505

Mamun A. A., Cairns R.A. 1996, Phys. Plasmas, 3, 702

Manesh M., Gopinathan S., Sebastian S., Willington N.T., Varghese A., Gangadharan R., Venugopal C. 2015, J. Appl. Math. Phys., 3, 1431

Manesh M., Neethu, T. W. Neethu J., Sijo S., Sreekala G., Venugopal C., 2016, J. Theor. Appl. Phys., 10, 289

Melandso F., Aslaksen T. K., Havens O. 1993a, J. Geophys. Res., 98, 13315

Melandso F., Aslaksen T., Havnes O. 1993b, Planet. Sp. Sci., 41, 321

Merlino R. L. 2014, J. Plasma Phys., 80, 773

Moghadam S. S., Dorranian D. 2013, Adv. Mater. Sci. Eng., Article ID 389365

Naeem I., Ehsan Z., Mirza A. M., Murtaza G., 2020, arXiv: 2001.09374v1

Oberc P., Parzydło W., Kopersk P., Klimov S. 1989, Adv. Sp. Res., 9, 347

Omidi N., Winske D., 1986, Geophys. Res. Lett., 13, 397

Pakzad H. R. 2009a, Chaos, Solitons and Fractals, 42, 874

Pakzad H. R. 2009b, J. Plasma Fus. Res. Series, 8, 261

Pakzad H. R. 2010, Pramana, 74, 605

Pakzad H. R., Javidan K. 2008, J. Phys. Conf. Series, 96, 012145

Rao N. N., Shukla P. K. 1994, Planet. Sp. Sci., 42, 221

Rao N. N., Shukla P. K., Yu M.Y. 1990, Planet. Sp. Sci., 38, 543

Rosenberg M. 1993, Planet. Space Sci., 41, 229

Rosenberg M. 1996, J. Vacuum Sci. Tech. A, 14, 631

Roussel-Dupre R. 1980, Sol. Phys., 68, 243

Rubin M., Hansen K. C., Gombosi T. I., Combi M. R., Altwegg K., Balsiger H. 2009, Icarus, 199, 505

Saini N. S., Kaur N., Gill T. S. 2015, Adv. Sp. Res., 55, 2873

Shahein R. A., Seadawy A. R. 2019, Ind. J. Phys., 93, 941

Shukla P. K., Mamun A. A., 2002, Introduction to Dusty Plasma Physics, IOP Publishing, London

Tribeche, M., Bacha, M. 2010, Phys. Plasmas 17 073701
Tribeche, M., Bacha, M., 2013, Phys. Plasmas 20 103704
Varma R. K., Shukla P. K., Krishnan V. 1993, Phys. Rev. E, 47, 3612
Verheest F. 1992, Planet. Sp. Sci., 40, 1
Washimi H., Taniuti T. 1966, Phys. Rev. Lett., 17, 996
Xie B., He K., Huang Z. 1998, Phys. Lett. A., 247, 403
Xie B., He K., Huang Z. 1999, Phys. Plasmas, 6, 3808